Improvement of the Interfacial Adhesion Between PBO Fibers and PPESK Matrices Using Plasma-Induced Coating

Xiangyi Zhang,[1] Ping Chen,[1,2] Xiaotao Kang,[1] Mingxin Chen,[1] Qian Wang[1]

[1]State Key Laboratory of Fine Chemicals, School of Chemical Engineering, Dalian University of Technology, Dalian 116023, China
[2]Liaoning Key Laboratory of Advanced Polymer Matrix Composites Manufacturing Technology, Shenyang University of Aeronautical and Astronautics, Shenyang 110136, China

ABSTRACT: This work deals with the plasma-induced coating process on the surface of PBO fibers to obtain a strong interfacial adhesion between the poly(p-phenylene benzobisoxazole) (PBO) fibers and the poly(phthalazinone ether sulfone ketone) (PPESK) matrices. The process consisted of four steps: (a) plasma preactivation of PBO fibers; (b) immersion in an epoxy resin solution; (c) drying and then soaking with the PPESK solution; (d) shaped by compression molding technique. The orthogonal experiments used in this study enable the determination of the significant experimental parameters that influence efficiency of the process by comparing the values of ILSS. The order of their influences was the concentration > power > treating time > treating pressure. The results of the interlaminar shear strength (ILSS) and water absorption showed that the ILSS of the composite increased by 56.5% after coating, meanwhile the water absorption declined to 0.32%. The changes of the surface chemical composition, the surface morphology, and the surface free energy of fibers were studied by FTIR spectroscopy, atomic force microscope (AFM), and dynamic contact angle analysis (DCAA), respectively. Fracture mechanism of the composite was examined by scanning electron microscope (SEM). The results indicated that plasma-induced coating process was an efficient method to enhance the interfacial adhesion of PBO fibers and PPESK matrices. © 2011 Wiley Periodicals, Inc. J Appl Polym Sci 123: 2945–2951, 2012

Key words: PBO fiber; plasma-induced coating; orthogonal experiment; interfacial adhesion; SEM

INTRODUCTION

Composites, which contain two or even more separate materials, combined with a macroscopic structural unit, have excellent properties.[1] Nowadays, polymer composites have been extensively used in high-performance polymer products.[2] The rigid rod polymeric fiber poly(p-phenylene benzobisoxazole) (PBO), which belongs to a new class of high performance "rigid-rod" PBZ materials, contains aromatic hetero-cyclic rings which provide fine chemical resistance and ensure good tensile.[3–7] Owing to its salient thermal stability, environmental resistance and specific stiffness and strength, PBO provides great potential applications as reinforcement fibers for composites. Therefore, PBO fibers have attracted great attention and have been extensively studied due to its applications in many areas such as aeronautical and aerospace applications, protective garments, and personal ballistic armors.[8]

However, it is a challenging issue to strengthen the adhesion between PBO fibers and matrices because of the relatively smooth and chemically inactive fiber surfaces which prevent efficient chemical and physical bonding at the interface.[9,10] Numerous researchers have paid full attention to the improvement of the interfacial adhesion which is believed to play an important role in composite properties. Various techniques, such as oxidation methods,[11] plasma modification,[12] γ-ray irradiation,[13] and modification through coupling agents,[14] have developed to introduce appropriate functional groups onto the fiber surfaces and modify the surface morphologies. Among the methods of surface modification, plasma treatment is most widely used. Plasma, which contains a significant concentration of cations and electrons, is a quasi-neutral gas stream and neutral particles that exhibit collective behavior. These charged particles can activate or react with a substrate surface.[15] Modification of polymer surfaces can be rapidly and cleanly achieved by plasma treatment due to the possibility of the formation of various active species on the surfaces of the fibers. Plasma treatment also results in the deposition of a
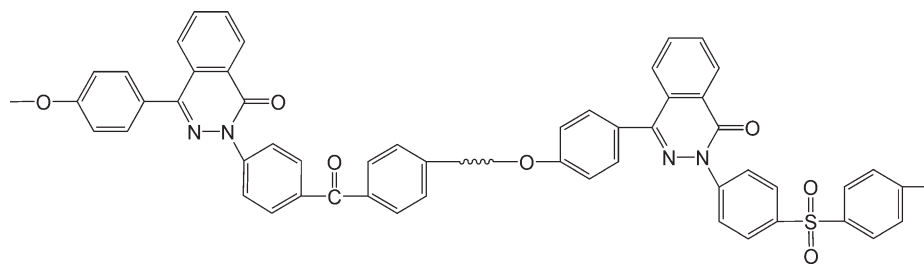
Figure 1 The chemical structure of PPESK.

macromolecular structure, graft polymerization, functionalization, etching, roughening, and crosslinking.[16] Plasma modification techniques have great advantages, such as environment friendly and low energy consumption.[17] Especially, plasma treatment can effectively increase the surface energy of a polymer without altering the bulk structure of the polymer.[18] Thus, in recent years, this technique is intensively undertaken in the treatment of polymers.[19]

In recent years, thermoplastic-matrix composites have gained increasing attention owing to their higher damage tolerance, higher heat resistance and so on. Poly(phthalazinone ether sulfone ketone) (PPESK) is a type of novel thermoplastic resin which exhibits excellent mechanical properties, thermo resistance, high damage tolerance, and good solubility compared with the traditional thermoplastic resins such as poly(ether ether ketone) (PEEK), poly(ether sulfone) (PES), and poly(ether imide) (PEI). The chemical structure of PPESK is shown in Figure 1. It can be dissolved in usual solvents such as *N,N*-dimethylacetamide (DMAc), *N*-methyl-2-pyrrolidone (NMP), and chloroform. Therefore, the solution impregnation technique can be used conveniently in the preparation of fiber-reinforced PPESK composites.[20]

The influences of oxygen plasma treatment time and treatment power on the surface properties of PBO fibers have been studied in previous work.[21,22] In this work, epoxy resin was used as a coating to obtain strong adhesion between PBO fiber and PPESK. The interlaminar shear strength (ILSS) and water absorption were measured to evaluate the strength of interfacial adhesion. Then the main factors of the process were investigated by an orthogonal experiment comparing the values of ILSS. The surface chemical composition of the fibers, the surface morphologies of the fibers, and the surface free energy of the fibers were studied by FTIR spectroscopy, AFM, and dynamic contact angle analysis (DCAA), respectively. Fracture mechanism of the composite was examined by SEM.

EXPERIMENTAL

Materials

PBO fiber was purchased as high modulus (HM) yarn from Toyobo Co. Ltd, Japan. The fibers were washed successively in acetone and distilled water at room temperature. Each step took about 24 h to remove surface sizing or contaminants. The fiber samples were then dried at 120°C in a vacuum oven for 3 h prior to the plasma treatment. The thermoplastic resin PPESK, characteristic viscosity of which was 0.48 and the glass transition temperature was 284°C, was supplied by Dalian Polymer New Material, China. The solvent was DMAc and the solution concentration is 13 wt % to get an appropriate fiber volume fraction. The epoxy resin bought from Dalian Qihua Chemical, is a kind of diglycidyl ether of bisphenol A (DGEBA) epoxy resin (the epoxy value is 0.51, and the epoxy equivalent is 196.1), which could be easily dissolved in acetone.

Plasma-induced coating

The plasma was carried out in an inductively coupled radio frequency (13.56 MHz) generator. The treatment system consisted of a vacuum chamber, three mass flow controllers, a pumping system, a pressure gauge, and a radio frequency source. Oxygen was fed into the vacuum chamber at a flow rate of about 30–40 SCCM. Fibers were rolled on a glass frame and fixed in a quartz obturator with 30 cm in height and 26 cm in inner diameter. The orthogonal experiment considered four experimental factors which may impact the ILSS value, i.e., the plasma power, operating pressure, treating time, and the concentration of the epoxy resin, which varied on three respectively, different levels. After the experimental factors and corresponding varied levels had been determined, the orthogonal table [noted as L_9 (3^4)] could then be chosen as the experimental scheme, which would denote the different assorted experimental programs and would greatly decrease the times of experiments, shown as Table I, where nine was the total number of experiments, three was the number of levels, and four was the factors number. Each experiment followed the same experimental procedure.

Composite specimen preparation

PBO fiber-reinforced PPESK composite was prepared by solution impregnation technique, which was described in Ref. [23] PPESK resin was dissolved in DMAc solvent (13%) and epoxy resin was dissolved

TABLE I
The Analysis of the Orthogonal Experiment

| | Factors | | | | |
Levels	Power (W)	Time (min)	Pressure (Pa)	Concentration (%)	ILSS (MPa)
1	50	5	10	1	39.4 (2.0)
2	50	10	30	3	51.1 (2.2)
3	50	15	50	5	50.1 (2.0)
4	100	5	30	5	43.2 (4.0)
5	100	10	50	1	44.0 (2.5)
6	100	15	10	3	44.7 (2.5)
7	200	5	50	3	47.8 (4.1)
8	200	10	10	5	46.1 (1.7)
9	200	15	30	1	38.0 (1.3)
Mean value 1	46.9	43.5	43.4	40.5	
Mean value 2	44.0	47.1	44.1	47.9	
Mean value 3	44.0	47.0	47.3	46.5	
Range	3.9	3.6	3.2	7.4	

Standard deviations are in parentheses.

in acetone with series of concentrations (to the weight of epoxy resin) according to the orthogonal plan. The freshly treated fibers were soaked in the epoxy/acetone solution for 12 h at a temperature of 25°C. Then the fibers were dried to vaporize acetone solvent. After that the fibers were soaked with the PPESK/DMAc solution. The monolayer impregnating samples were performed to vaporize DMAc solvent and then shaped by compression molding technique.

ILSS

ILSS was measured to estimate the interfacial adhesion strength of the composite. The ILSS data were obtained in a three-point short-beam bending test method on a Schimadzu universal testing machine according to GB3357-82. The specimens were cut at the dimensions of $25 \times 6 \times 2$ mm^3, and the ratio of the span to thickness was five. Each ILSS value reported was the average of five successful measurements. The specimens were tested at a constant crosshead movement rate of 2 mm/min. ILSS, τ, was calculated according to the following expression:

$$\tau = \frac{3 P_b}{4b \bullet h} \qquad (1)$$

where τ is the interlaminar shear strength in MPa, P_b the maximum compression load at fracture in Newton, b the width of the specimen in millimeters, and h the thickness of the specimen in millimeters.

Water absorption

Water absorption test has been done to investigate the interfacial properties of PBO fiber-reinforced

PPESK composite. The experiment was carried out according to the ASTM D-570 method. Percentage of water absorption can be calculated to the nearest 0.01% as follows:

$$\text{Water absorption}(\%) = \frac{m_w - m_c}{m_w} \times 100\% \qquad (2)$$

where m_w and m_c stand for the wet weight and conditioned weight of the composite specimens, respectively.

FTIR

The relative amount of epoxy coatings on the PBO fiber was examined by diffuse reflectance fourier transform infrared spectroscopy (FTIR) method. FTIR spectra were obtained in an NEXUS IR system which was manufactured in America. FTIR scans were performed in reflectance mode applying a wavenumber range of 2000 to 700 cm^{-1} with the wavenumber resolution of 2 cm^{-1}, and the average result of 32 automatic scans was output as the test result. The epoxy resin was used without any curing agent.

AFM

The effects of plasma-induced coating on fiber surface morphology and surface roughness were analyzed by AFM in the tapping mode (Picoplus II, Agilent). A single fiber was fastened to a steel sample mount. Morphology images were simultaneously recorded for each fiber on various scanned areas (4 µm × 4 µm). The surface roughness was evaluated by R_q, short for root mean-square, and R_a, short for arithmetic mean roughness, calculated from eqs. (3) and (4) using the AFM software.

$$R_q = \sqrt{\frac{1}{N^2} \sum_{i=1}^{N} \sum_{j=1}^{N} (z_{ij} - z_{av})^2} \qquad (3)$$

$$R_a = \frac{1}{N} \sum_{i=1}^{N} \sum_{j=1}^{N} |z_{ij} - z_{cp}| \qquad (4)$$

where N is the number of data points in the image, i and j are the pixel locations on the AFM image, z_{ij} is the height at i and j locations, z_{av} is the average height value within the given area and z_{cp} is the height value from the center plane.

DCAA

The values of surface free energy of uncoated and coated PBO fiber were analyzed according to Wihelmy method, on a dynamic contact angle analysis system (DCA-322, Thermo Cahn). The fiber sample was cut

into about 1 cm in length and mounted indirectly to a wire hook suspending from microbalance and then immersed into the testing liquid media by elevating the stage at a constant speed of 1 mm/min. The contact angles (θ) were calculated using a computer system from eq. (5).

$$F = \gamma \cdot p \cdot \cos\theta \qquad (5)$$

where F is the wetting force between the fiber and the testing liquid, which is measured by the microbalance; γ is the surface tension of the testing liquids; p the wetted perimeter; θ the contact angle between fiber and liquid.

Fiber surface free energy, which can be divided into two components: dispersive and polar, were derived from eqs. (6) and (7).

$$\gamma_l(1 + \cos\theta) = 2 \cdot \sqrt{\gamma_s^p \gamma_l^p} + 2 \cdot \sqrt{\gamma_s^d \gamma_l^d} \qquad (6)$$

$$\gamma_{\text{Total}} = \gamma_s^p + \gamma_s^d \qquad (7)$$

where γ_1 is the surface tension of the testing liquid, γ_{Total} the surface free energy of the fiber, γ_s^p the polar component, and γ_s^d the dispersive component.[24]

The testing liquids used in the measurement were water (polar solvent) and diiodomethane (nonpolar solvent), their surface tensions were 72.3 mN/m and 50.8 mN/m, respectively.

SEM

To analyze the fracture mechanism of the composite, SEM (QUANTA 200, FEI) was applied to observe the morphologies of the shear ruptures of composite interlaminar. The chamber's pressure was evacuated to a pressure less than 60 Pa using a molecular pump. The fracture composite surfaces were examined and the magnification of the image for the composite interlaminar shear rupture was set at 1000×.

RESULTS AND DISCUSSION

The influence of plasma-induced coating on the interfacial adhesion of composite

It is well known that the mechanical properties depend on the properties of the interface of a composite. ILSS is a central method for signifying composite interfacial adhesion property. The method to process the orthogonal experimental data was very important because the experimental times had been greatly reduced. One of the aims of the orthogonal experiments was to find the optimum matching of the four factors. The second aim was to detect the most important experimental factor on the properties of the composites, especially on the ILSS.[25] Therefore, we analyzed the orthogonal experiment by comparing the values of ILSS, which was shown in Table I, and each data of ILSS entry was the average of five successful measurements. The standard deviations were also given in the parentheses.

Based on the mathematical statistics theory, if the experimental values at the same level in the orthogonal experiments for each experimental factor were added together and then were divided by three (the number of the levels), the average value at the same level for each experimental factor was attained. Then the range, which was the maximum value minus the minimum value of the experimental average value, was calculated. The range analysis could discriminate the relative importance of each factor. According to the range analysis on the ILSS, the important influencing factors were the concentration, power, treating time, treating pressure, in sequence. In other words, the concentration of the epoxy resin had the most sensitive effect on the ILSS. This result indicated that the new polymeric layer should have an appropriate thickness, and much work needed to be done to reveal the relationship between the thickness of the coating and the properties of the composites. As a consequence, the optimal process parameters of the process we would choose are shown in Table I and the specimens used in other tests were all manufactured according to this process, due to the best ILSS results which were obtained by it.

The interfacial adhesion was also examined by the percentage of water absorption, which was shown in Table II. It was found that the ILSS and water absorption of the untreated composite were 32.67 MPa and 0.44%, respectively, as we had reported in Ref. [26]. After plasma-induced coating, the ILSS of the composite increased to 51.14 MPa with a 56.5% increase while the water absorption declined to 0.32%.

As we know, a strong interfacial adhesion between the fiber and the matrix could be an effective obstacle to water permeating into the composite. Both ILSS test and water absorption test indicated that plasma-induced coating was an effective method to improve the interfacial adhesion between the PBO fiber and PPESK matrix significantly.

TABLE II
The ILSS Values and Water Absorption of PBO Fiber-Reinforced PPESK Composite

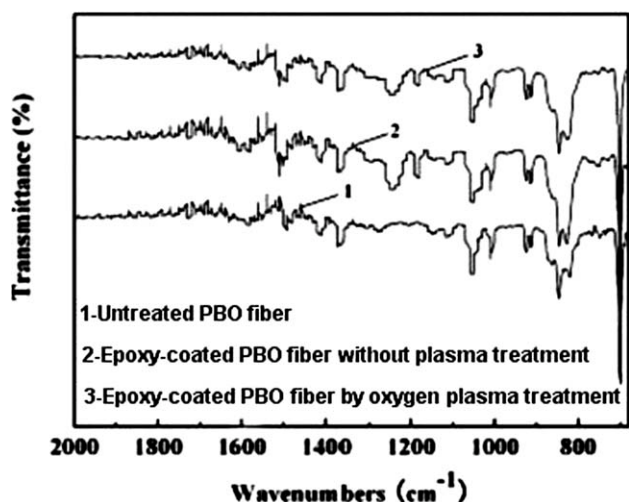| Samples	ILSS (MPa)	Water absorption (%)
Untreated	32.67 (0.7)	0.44
Plasma-coated	51.14 (2.2)	0.32

Standard deviations are in parentheses.

Figure 2 FTIR spectra of PBO fibers before and after plasma-coated-epoxy modification.

The changes of the epoxy resin during the plasma treatment

To investigate the possible change of chemical composition of the PBO fibers before and after plasma-induced coating, FTIR spectroscopy measurements are performed. As Figure 2 depicts, the absorption band of C—O—C group at 913 cm^{-1} gradually reduced in intensity in the order of 2, 3, and 1. The occurrence phenomenon confirms that plasma can initiate the cure reaction of the epoxy resin. We measured the relative residual functional band ratio to compare the characteristics of this system before and after treatment, as follows:

$$\alpha = \frac{\frac{A_{913}}{A_{700_{(G_0)}}} - \frac{A_{913}}{A_{700_{(G_1)}}}}{\frac{A_{913}}{A_{700_{(G_0)}}} - \frac{A_{913}}{A_{700_{(0)}}}} \times 100\% \tag{8}$$

where A_{913} is the area of the absorption band at 913 cm^{-1}, A_{700} represents the area of the absorption band at 700 cm^{-1} represented aromatic skeletal ring breathing vibration mode, which is not changed during the treatment. And the values of the α is 60.20%.

These results clearly indicated that the plasma treatment could make the PBO have an interaction with epoxy resin, and then a new polymeric layer was formed which could improve the adhesion between the fiber and matrix. The possible interaction mechanism was illustrated by Park et al.[27] There were two interfaces in this case: one interface can be between the fiber and the epoxy resin while the other can be between the epoxy resin and the matrix. At the two interfaces, either primary or secondary bonds can exist between PBO fiber or PPESK matrix and epoxy resin. These primary or secondary bondings may contribute to improve the interfacial adhesion.[27]

The changes of morphologies by AFM

It is well known that the adhesion properties of the interface between the fiber and the matrix not only depend on chemical effects but also relate to physical effects, thus the evaluation of surface morphology and surface roughness is significant in our discussions.[28] AFM was used for observing the surface morphologies in this study and measuring the surface roughness. Figure 3 shows the three-dimensional morphology AFM images of the surfaces of untreated and plasma-coated PBO fibers.

By comparing the three-dimensional AFM morphology images, it can be seen that plasma-induced coating could change the surface morphology on a microscopic scale. The surface of the untreated fibers shown in Figure 3(a) was quite smooth and had a few shallow grooves. The R_a was 240.2 Å and R_q was 263.5 Å for the untreated sample. However, as we can see from Figure 3(b) which revealed the surface roughness of plasma-induced-coated PBO fiber, there were several remarkable grooves possibly caused by plasma-induced coating. The R_a was 569.8 Å and R_q was 613.3 Å for the plasma-coated sample, which was much higher than the values of untreated one.
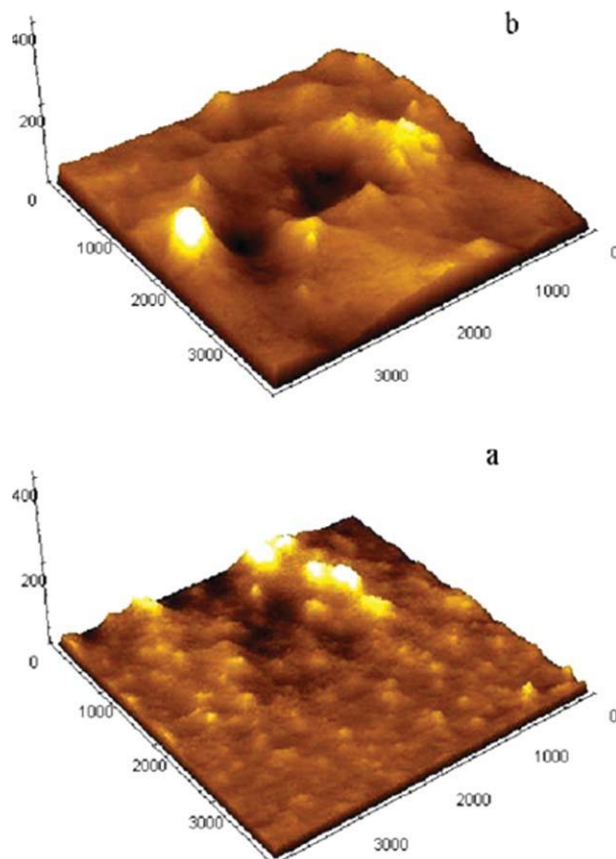

Figure 3 AFM morphologies of PBO fibers: (a) untreated; (b) plasma-induced-coated. [Color figure can be viewed in the online issue, which is available at wileyonlinelibrary.com.]

TABLE III
Contact Angles and Surface Free Energies of PBO Fibers of Untreated and Coated

samples	Contact angles $(\theta) \pm$ s.d. (°)		Surface free energy (mJ/m^2)		
	Water	Diiodomethane	γ^p	γ^d	$\gamma_{Total} = \gamma^p + \gamma^d$
Untreated	76.6 ± 2.5	39.0 ± 1.7	5.48	40.11	45.59
Coated	71.4 ± 0.5	38.1 ± 1.5	7.57	40.55	48.12

s.d., Standard deviation.

The improvement of the surface roughness for the plasma-induced-coated fibers should be beneficial for their applications as a reinforcement in a composite system, and the reason may be that a rougher fiber morphology would provide more contact points and lead to a higher degree of mechanical interlocking between the fiber and the matrix.[29,30] In conclusion, plasma-induced coating can increase the roughness of the fiber surface, and then the adhesion of the fiber and resin will be improved in a large degree.

The changes of fiber surface free energy

It is well known that fiber wettability is the characterization of surface free energy which includes polar and dispersive components.[20] The surface free energy was analyzed from the measured contact angles which were obtained from each fiber sample contacted with two different liquids in our experiments. The surface energy components of the two testing liquids including distilled water and diiodomethane are 72.3 mJ/m² and 50.8 mJ/m², respectively. The surface wettability of fibers untreated and plasma-coated was examined by DCAA. The measured contact angles and the derived surface free energy of untreated and coated fibers were shown in Table III. The standard deviations were also given in the table, and each data entry was the average of five or more measurements. As shown in Table III, it is found that the PBO fiber surfaces become more hydrophilic after plasma-induced coating, which is shown by the dramatic decrease of the advancing water contact angle, θ_a, from 76.6° for untreated sample to 71.4° for plasma-coated one. From the measured contact angles between water or diiodomethane and PBO fiber, the surface free energy (γ_{Total}) is obtained. The γ_{Total} increased from 45.59 mJ/m² to 48.12 mJ/m² due to the polar functional groups introduced to the fiber surface. The results indicated that there was an increase of the fiber surface free energy. Combined with the results of AFM, it was also an evidence that the promotion of the interfacial adhesion was mainly caused by the increase of the fiber surface roughness.

The analysis of composite fracture mechanism

When composite suffers form load, the stress distribution on the fiber and matrix satisfies the Kelly-Tyson theory.[31,32] Based on the theory, the fracture modes will change according to the adhesive condition of interface between the fiber and the matrix. If there is a good interfacial adhesion, the rupture of composites will take place in matrix near the interface with a number of resin adhered to fiber surfaces. On the other hand, with poor interfacial adhesion the fracture mode will occur on the interface between the fiber and the matrix, and the fiber is clean with low amount of resin adhered on the surfaces.[20]

Figure 4 shows a schematic morphology of interlaminar shear ruptures of composites. It is found that the fibers are smooth with low amount of resin adhered to surface for the untreated specimen in Figure 4(a), so the rupture takes place on the
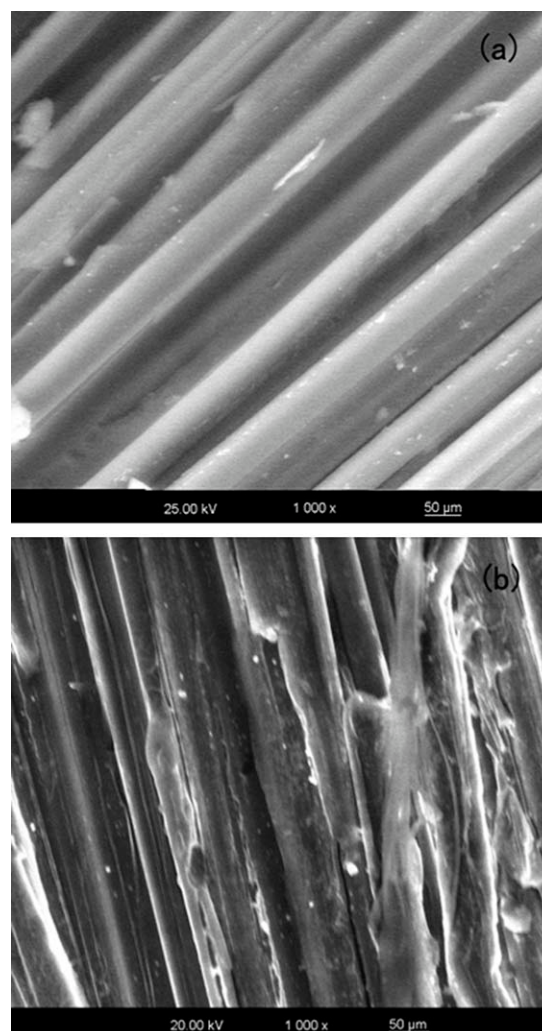

Figure 4 Fractured SEM photographs of PBO fiber reinforced PPESK composites: (a) untreated specimen; (b) plasma-coated specimen.

interface between fiber and matrix. However, a large proportion of fibers stick tightly to matrix, the primary failure mode varies from interface failure to matrix or fiber failure as shown in Figure 4(b). The SEM results confirmed that plasma-induced coating was an effective method to improve the interfacial adhesion by roughening the fiber surface which increased physical adhesion by mechanical interlocking between the fiber and its surrounding matrix. The results were in accord with the ILSS data. Combining the ILSS with the results of FTIR, AFM, and SEM, the improvement is partly because primary or secondary bonds were formed between the fiber and matrix by introducing a new polymeric layer, partly because the surface roughness of fiber was increased, which strengthen mechanical interlocking between the fiber and the matrix.[26]

CONCLUSIONS

In this work, we studied the process of plasma-induced coating which aimed at improving the interfacial adhesion between PBO fiber and PPESK resin. The ILSS and water absorption tests showed that PBO fibers with epoxy resin coating could improve the interfacial adhesion in a composite system. Through the range analysis on the orthogonal experiment results, the most important factor influencing the ILSS was the concentration of the epoxy resin and 3% was the optimum. FTIR provided a proof that plasma treatment made PBO has an interaction with the epoxy resin and a new polymeric layer was formed. AFM results suggested that plasma coating could increase the surface roughness in a large degree, which may increase the mechanical interlocking between the fibers and the matrices. DCAA tests showed that epoxy coating could improve the wettability of the fiber, but the changes of the surface free energy were not in a large degree. The main reason for the promotion of interfacial adhesion was the increase of the mechanical interlocking. Composite fracture SEM photographs illustrated that the primary failure mode of composites changed from interface failure to matrix failure after plasma-induced coating. In conclusion, plasma-induced coating may be a useful way to improve the interfacial adhesion of PBO fiber and PPESK resin. The interaction mechanism was an important issue in the study of interfacial behavior, in light of these considerations, it is hoped that the findings of this study provide a firm basis on which to undertake additional research work.

References

1. Gibson, R. F. Principles of Composite Material Mechanics; McGraw-Hill, Inc: New York, 1994.
2. Sugihara, H.; Jones, F. R. Polym Compos 2002, 30, 318.
3. Hu, X. D.; Jekins, S. E.; Min, B. G.; Polk, M. B.; Kumar, S. Macromol Mater Eng 2003, 288, 823.
4. Bourbigot, S.; Flamebard, X. Fire Mater 2002, 26, 155.
5. Kitagawa, T.; Yabuki, K.; Young, R. J. Polymer 2001, 42, 2101.
6. Kitagawa, T.; Murase, H.; Yabuki, K. J Polym Sci Part B: Polym Phys 1998, 36, 39.
7. Chae, H. G.; Kumar, S. J Appl Polym Sci 2006, 100, 791.
8. Zhang, C. S.; Chen, P.; Liu, D.; Wang, B. C.; Li, W.; Kang, X. T. Surf Interface Anal 2009, 41, 187.
9. Bourbigot, S.; Flambard, X.; Revel, B. Eur Polym J 2002, 38, 1645.
10. Kitagawa, T.; Ishitobi, M.; Yabuki, K. J Polym Sci Part B: Polym Phys 2000, 38, 1605.
11. Wu, G. M.; Huang, C. H.; You, J. H.; Liu, S. J. J Polym Res B 2004, 11, 31.
12. Mäder, E.; Melcher, S.; Liu, J. W.; Gao, S. L.; Bianchi, A. D.; Zherlitsyn, S.; Wosnitza, J. J Mater Sci 2007, 42, 8047.
13. Zhang, C. H.; Huang, Y. D.; Zhao, Y. D. Mater Chem Phys 2005, 92, 245.
14. Liu, D. D.; Hu, J.; Zhao, Y. M.; Zhou, X. S.; Ning, P.; Wang, Y. J Appl Poly Sci 2006, 102, 1428.
15. Wu, G. M. Mater Chem Phys 2004, 85, 81.
16. Kato, K.; Uchida, E.; Kang, E.-T.; Uyama, Y.; Ikada, Y. Prog Polym Sci 2003, 28, 209.
17. De Geyter, N.; Morent, R.; Leys, C. Surf Coat Technol 2006, 201, 1117.
18. Li, C. L.; Tu, C. Y.; Huang, J. S.; Liu, Y. L.; Lee, K. R.; Lai, J. Y. Surf Coat Technol 2006, 201, 63.
19. Borcia, G.; Anderson, C. A.; Brown, N. M. D. Surf Coat Technol 2006, 201, 3074.
20. Chen, P.; Lu, C.; Yu, Q.; Gao, Y.; Li, J. F.; Li, X. L. J Appl Polym Sci 2006, 102, 2544.
21. Zhang, C. S.; Chen, P.; Sun, B. L.; Li, W.; Wang, B. C.; Wang, J. Appl Surf Sci 2008, 254, 5776.
22. Chen, P.; Zhang, C. S.; Zhang, X. Y.; Wang, B. C.; Li, W.; Lei, Q. Q. Appl Surf Sci 2008, 255, 3153.
23. Chen, P.; Zhang, C. S.; Wang, J. China Pat. ZL200610134662.3. 2009.
24. Lu, C.; Chen, P.; Yu, Q.; Ding, Z. F.; Lin, Z. W.; Li, W. J Appl Polym Sci 2007, 106, 1733.
25. Zhong, J. H.; Qing, L.; Zheng, L. Y.; Qiang, L. Energy Conversion Manage 2008, 49, 1211.
26. Zhang, C. S.; Chen, P.; Sun, B. L.; Lu, C.; Zhang, X. Y.; Liu, D. J Appl Polym Sci 2009, 113, 71.
27. Park, J. M.; Kim, D. S.; Kim, S. R. J Colloid Interface Sci 2003, 264, 431.
28. Wang, J.; Chen, P.; Li, H.; Zhang, C. S.; Sun, B. L.; Zhang, X. Y. Surf Coat Technol 2008, 202, 4986.
29. Cioffi, M. O. H.; Voorwald, H. J. C.; Hein, L. R. O.; Amberosio, L. Compos A 2005, 36, 615.
30. Cvelbar, U.; Pejovnic, S.; Mozetie, M.; Zalar, A. Appl Surf Sci 2003, 210, 255.
31. Vlasveld, D. P. N.; Parlevliet, P. P.; Bersee, H. E. N. Compos A 2005, 36, 1.
32. Ye, L.; Afaghi-Khatibi, A.; Lawcock, G. Compos A 1998, 29, 1525.